

## Flexural rigidity characteristics of light-weighted mirrors

Pravin K. Mehta

Optical Group Research, Perkin-Elmer Corporation  
Mail Station 848  
100 Wooster Heights Road, Danbury, Connecticut, 06810-7589

### Abstract

One of the key parameters usually considered in a light weighted mirror design is its flexural rigidity. In part I of this paper, the relative merits of symmetric sandwich and open back light-weighted designs in the 10 to 30 kg/m<sup>2</sup> range (of mirror weight per unit area) are examined for ULE, Heraeus fused silica, Zerodur and beryllium, subject to some representative state-of-the-art fabrication constraints. Part II of the paper addresses the same issue independently of any specific material. This is made possible by normalization of several parameters by the weight equivalent solid thickness of the mirror. Also included in the study are nonsymmetric sandwich cross sections with unequal front and rear facesheet thicknesses. The study shows that, for given values of mirror weight per unit area and the core (or rib) solidity ratio, there exists a transitional value of the normalized front facesheet thickness above which an open back configuration is structurally superior to a sandwich configuration. Moreover, for the increasingly demanding light-weighting goals of modern optical systems, the optimum geometrical configurations may be beyond the fabrication capability of the current state of the art.

### Introduction

The objective of light-weighting a mirror is to improve its structural efficiency. In many applications, this means, for a specified value of mirror weight per unit area, the maximization of its flexural rigidity subject to state-of-the-art fabrication constraints. Thus, the flexural rigidity of a light-weighted mirror, shown schematically in Figure 1, may be considered as a representative relative stiffness parameter for such applications, because the higher the flexural rigidity, the smaller is the flexural deformation due to given nonthermal loads. On the other hand, for minimum thermal bowing of the mirror, the parameter  $M_t/D$ , where  $M_t$  is the thermal moment, should be minimized. This parameter, being dependent on the actual thermal loading of the mirror, is considered to be out of scope of this study.

The details of lightweighted sandwich core design and the openback rib structure are essentially not required in the flexural rigidity calculations, provided that the core or rib cell size is small in comparison with the mirror diameter. The core and rib structures may then be treated as homogeneous, isotropic solids of reduced effective elastic moduli, proportional to  $\kappa\eta$ , where  $\kappa$  = core (or rib) effectiveness factor and  $\eta$  = core (or rib) density or solidity ratio (See Appendix A). Some commonly used rib patterns are illustrated in Figure 2. The effectiveness factor for square and triangular patterns is 0.5, while that for the hexagonal patterns may be significantly smaller. The study is applicable to any homogeneous linear elastic material.

### Notation

A = Area of the mirror  
D = Flexural rigidity of light-weighted section  
D<sub>s</sub> = Flexural rigidity of weight equivalent solid section  
E = Young's modulus  
I = Moment of inertia of light-weighted section  
I<sub>s</sub> = Moment of inertia of weight equivalent solid section  
M<sub>t</sub> = Thermal moment (for bowing)  
W = Mirror weight  
b = diameter of the inscribed circle  
b<sub>c</sub> = center to center rib spacing  
b<sub>h</sub> = length of the side of a hexagon

b<sub>s</sub> = length of the side of a square  
b<sub>t</sub> = length of the side of an equilateral triangle  
c<sub>f</sub> = Distance of neutral surface from the front surface  
h<sub>c</sub> = Core depth or rib height  
m = 1 for openback section  
= 2 for sandwich section  
t<sub>b</sub> = Equivalent bending thickness  
t<sub>f</sub> = Front facesheet thickness  
t<sub>r</sub> = Rear facesheet thickness  
t<sub>s</sub> = Weight equivalent solid thickness  
t<sub>w</sub> = rib thickness  
ρ = Weight density  
ν = Poisson's ratio  
β = Normalized front facesheet thickness  
β<sub>0</sub> = Optimum value of β  
β<sub>t</sub> = Transitional value of β  
γ = Normalized flexural rigidity  
μ = Rear facesheet thickness ratio  
η = Core or rib solidity ratio  
κ = Core or rib effectiveness factor

Several other symbols, mainly used for convenient abbreviation of mathematical expressions, are defined later when they are introduced in the text.

### Part I : State-of-the-Art Light-Weighted Mirrors

This part deals with a study of the relative merits of symmetric sandwich and openback concepts of mirror light-weighting for maximizing flexural rigidity of the section subject to some representative state-of-the-art fabrication constraints on facesheet thickness. Four mirror materials are considered in the study: ULE, Zerodur, Heraeus fused silica and beryllium. Their mechanical properties are given in Table 1, while the state-of-the-art fabrication constraints on minimum facesheet thickness and core density based on current experience are given in Table 2. For each of these values of minimum facesheet thickness, the core or rib density is parametrically varied between 0.04 and 0.10 in step increments of 0.01. This range of core density includes the minimum  $\eta$  values of Table 2.

**Table 1 Mechanical Properties of Mirror Materials**

Material	E psi	$\nu$	$\rho$ lb/in <sup>3</sup>
ULE	98 x 10 <sup>6</sup>	0.17	0.080
Zerodur	136 x 10 <sup>6</sup>	0.24	0.091
Fused Silica (Heraeus)	101 x 10 <sup>6</sup>	0.17	0.080
Beryllium	420 x 10 <sup>6</sup>	0.08	0.067

**Table 2 State-of-the-art Fabrication Constraints**

Material	Minimum $t_f$ inch	Minimum $\eta$ %	Core (rib) fabrication process
ULE	0.25	6.0	Fritting
Zerodur	0.12	7.5	Fusing
Fused Silica (Heraeus)	0.12	4.0	Extrusion tubing
Beryllium	0.08	7.5	HIP *

\* Hot Isostatic Pressing

**Limit of Light-weighting**

For any given weight per unit area, or W/A, there is a fixed amount of material, from which the light-weighted design is to be fashioned. From this amount, the facesheet of an openback design takes a share, which is at least equal to the minimum  $t_f$  value given in Table 2. For the symmetric sandwich design, this minimum share is  $2t_f$ , because there is a facesheet also in the back of the mirror. The balance of the material can be used for fabricating the light-weighted core or rib structure. The greater the core or rib depth  $h_c$ , the farther is the facesheet from the neutral axis, and the greater is the flexural rigidity. For calculating  $h_c$ , consider the mirror weight given by

$$W = \rho A(mt_f + \eta h_c) \tag{1}$$

From this,

$$h_c = (W/\rho A - mt_f)/\eta \tag{2}$$

Thus for a given value of  $t_f$ , the core or rib depth varies linearly with W/A and inversely with  $\eta$ . Using the minimum values of  $t_f$  from Table 2,  $h_c$  is plotted in Figures 3 through 6 against W/A with a parametric variation of  $\eta$  for various materials under consideration. It can be observed that

- for a given W/A, the openback rib height is greater than the sandwich core depth
- $h_c$  increases with decrease in core or rib density

- $h_c$  becomes zero in some cases in the 10 to 30 kg/m<sup>2</sup> range of W/A

When  $h_c$  becomes zero, all the available material is required for the facesheets. This defines the limit of light-weighting. With  $h_c$  equal to zero, formula (2) yields  $mt_f = W/\rho A$ . This is the weight-equivalent solid thickness  $t_s$ , which is plotted in Figure 7 vs mirror weight per unit area. From this plot, it can be observed that

- no practical ULE sandwich design is feasible below 30 kg/m<sup>2</sup> within the current state-of-the-art fabrication technology, while the openback lightweighting is limited to greater than 15 kg/m<sup>2</sup>
- for Heraeus fused silica and Zerodur, sandwich construction is not feasible below 16 and 18 kg/m<sup>2</sup>, respectively, while the openback designs are feasible for both down to 10 kg/m<sup>2</sup>
- only for beryllium, both types of light-weighting are feasible down to 10 kg/m<sup>2</sup>

The numerical values of W/A at which light-weighting becomes mathematically impossible for the assumed fabrication constraints are summarized in Table 3.

**Table 3 Limiting Values of W/A at which Light-weighting becomes mathematically impossible**

Material	Minimum W/A, Kg/m <sup>2</sup>	
	Sandwich	Open Back
ULE	28.12	14.06
Zerodur	15.35	7.68
Fused Silica (Heraeus)	13.50	6.75
Beryllium	7.31	3.66

- For the assumed constraints on facesheet thickness, light-weighting is mathematically impossible at or below these values of W/A
- The working limits on W/A will be somewhat higher due to practical considerations such as meaningful core (or rib) height  $h_c$  relative to the facesheet thickness  $t_f$

**Flexural Rigidity**

The flexural rigidity of the symmetric sandwich and openback cross sections are given by

$$D = Et_b^3 / 12(1 - \nu^2), \tag{3}$$

where, for the symmetric sandwich section, we have

$$t_b^3 = (2t_f + h_c)^3 - (1 - \eta/2)h_c^3, \tag{4}$$

and, for the openback section, we have

$$t_b^3 = \left\{ \begin{aligned} & \{(1 - \eta/2)(t_f^4 - \eta h_c^4/2) \\ & + (t_f + h_c)^4 \eta/2\} / (t_f + \eta h_c/2) \end{aligned} \right\} \quad (5)$$

With  $E$ ,  $\nu$ ,  $\rho$  and  $t_f$  from Table 2 and  $h_c$  from formula (2), the flexural rigidities can be computed from formulas (3), (4) and (5). The results are plotted in Figures 8 through 11, from which the following main features can be observed

- For ULE (Figure 8), the openback construction is decisively superior to the symmetric sandwich construction in the 30 kg/m<sup>2</sup> class and below. It is at a significantly higher value of W/A, above which the sandwich design is better than the openback design.
- For Zerodur (Figure 9), the openback configuration is barely better at 30 kg/m<sup>2</sup>, but becomes increasingly better than the sandwich configuration with decrease in W/A. The trend is reversed in favor of the sandwich section not very far above 30 kg/m<sup>2</sup>.
- For Heraeus fused silica (Figure 10), the sandwich design is slightly better than the openback design at 30 kg/m<sup>2</sup>. The trend is reversed at approximately 27 kg/m<sup>2</sup>, below which the openback section becomes increasingly better than the sandwich section with decrease in W/A.
- For beryllium (Figure 11), the sandwich construction is somewhat better than the openback construction at 30 kg/m<sup>2</sup>. This small advantage gradually diminishes to zero at approximately 15 kg/m<sup>2</sup>, below which the openback design is increasingly superior to the sandwich design with decrease in W/A.

It can be surmised from these observations that, for every material, there exists a transitional value of W/A at which the flexural rigidities of the two types of light-weighted cross sections become equal for any given value of core or rib density  $\eta$ . This transitional value depends on the assumed state-of-the-art value of minimum facesheet thickness. Above the transition value of W/A, the sandwich

Table 4. Mirror Weight per Unit Area for Transition between Sandwich and Open Back Configurations

Material	$t_f$ inch	Transition W/A, Kg/m <sup>2</sup>	
		$\eta = 0.04$	$\eta = 0.10$
ULE	0.25	60.08	57.30
Zerodur	0.12	32.80	31.28
Fused Silica (Heraeus)	0.12	28.84	27.51
Beryllium	0.08	16.10	15.36

- At the transition W/A, the flexural rigidities of sandwich and open back sections are equal
- Above the transition W/A, the sandwich section has greater flexural rigidity than the open back section
- Below the transition W/A, the open back section has greater flexural rigidity than the sandwich section.

section is better than the openback section, and the difference between their flexural rigidities increases rather slowly with increase in W/A. Not only is the trend reversed below the transition value of W/A in favor of the openback section, but the difference between their flexural rigidities also grows rather rapidly with decrease in W/A. This happens because increasingly less material is available to the sandwich than the openback section to form the core (or rib) structure, as W/A decreases below the transition value. For convenience, the transition values of W/A are listed in Table 4.

Finally, for a given facesheet thickness and a given value of W/A, the flexural rigidity always increases with decrease in core (or rib) density  $\eta$ . This is due to the fact that the core (or rib) depth  $h_c$  increases with a decrease in  $\eta$  (Formula 2). There is always a price to pay for such an advantage. For instance, the transverse compressibility also increases with a decrease in  $\eta$ . A local web buckling problem may arise. The most difficult problem with decreasing  $\eta$  may be posed by fabrication constraints.

### Optimization

For a given value of mirror weight per unit area, a cross section with maximum flexural rigidity can be obtained by optimally distributing the available material between the facesheets and the core (or the rib) structure. The equation for optimum facesheet thickness is obtained by equating  $dD/dt_f$  to zero. By utilizing formulas (2) through (5), and performing the required differentiations and some algebraic manipulations, the following results are obtained

#### Optimum Symmetric Sandwich Section

$$t_f = \frac{W [\sqrt{(1 - \eta/2)} - \sqrt{(1 - \eta)}]}{\rho A [2\sqrt{(1 - \eta/2)} - \sqrt{(1 - \eta)^3}]} \quad (6)$$

#### Optimum Openback Section :

$$4(t_f + \eta h_c/2)\{(1 - \eta/2)(t_f^3 + h_c^3/2) + (\eta - 1)(t_f + h_c)^3/2\} - (1/2)\{(1 - \eta/2)(t_f^4 - \eta h_c^4/2) + \eta(t_f + h_c)^4/2\} = 0 \quad (7)$$

Substitution of  $h_c$  from (2) into (7) will yield a biquadratic equation in  $t_f$ , which can be numerically solved on a computer. By formula (6), as the core density  $\eta$  varies between 0.04 and 0.10, the optimum facesheet thickness for the symmetric sandwich section varies between  $0.1029W/\rho A$  and  $0.1075W/\rho A$ . From eq (7), the corresponding values obtained for the openback section are  $0.0964W/\rho A$  and  $0.1005W/\rho A$ . For the four materials under consideration, Figure 12 shows plots of  $t_f/(W/\rho A)$  vs W/A based on the fabrication limited facesheet thicknesses given in Table 2. Using the above ranges of optimum values of  $t_f$  for the openback and sandwich sections, it can be seen from this figure that none of the fabrication limited cross sections considered here in the 10 to 30 kg/m<sup>2</sup> range is optimum. Even in the extended range of W/A up to 55 kg/m<sup>2</sup>, only beryllium has the potential of providing optimum cross sections, when W/A is greater than 35 kg/m<sup>2</sup>.

### Conclusion

Based on the fabrication limited minimum facesheet requirement for every material,

- there is a limit for mirror weight per unit area, or W/A, below which no light-weighting is possible

- there exists a transitional value of  $W/A$ , at which the flexural rigidities of the openback and symmetric sandwich sections are equal. Below the transitional  $W/A$ , the openback design is superior to the sandwich design
- the achievable light-weighting is not optimum

## Part II : Normalized Flexural Rigidity Characteristics

In this part, the flexural rigidity characteristics of light-weighted mirrors are studied independently of any specific material. The required normalization is achieved by means of the weight-equivalent solid thickness  $t_s$ , which represents a fixed amount of material available for any given mirror weight per unit area, or  $W/A$ , and is given by

$$t_s = W/\rho A \quad (8)$$

The moment of inertia of the solid cross section per unit width is

$$I_s = t_s^3/12 \quad (9)$$

and the corresponding flexural rigidity is

$$D_s = EI_s/(1 - \nu^2) \quad (10)$$

These quantities for the weight equivalent solid cross section are used to normalize the corresponding quantities for the light-weighted cross section. Thus

$$\beta = t_f/t_s \quad (11)$$

$$\mu = t_r/t_f = t_r/\beta t_s \quad (12)$$

$$\gamma = D/D_s = I/I_s \quad (13)$$

The normalized flexural rigidity  $\gamma$  is, therefore, independent of material properties. For convenience, the flexural rigidity  $D_s$  of weight equivalent solid sections is given in Figure 13 in a graphical form as a function of mirror weight per unit area for several materials. Using this together with the  $t_s$  vs  $W/A$  plots of Figure 7, the facesheet thicknesses and flexural rigidity of a light-weighted section can be calculated from appropriate normalized charts given later in this paper.

### Limit of Light-weighting

Since the available material is divided among the front and rear facesheets and the core, we have

$$\left. \begin{aligned} t_s &= t_f + t_r + \eta h_c = t_f + \mu t_f + \eta h_c \\ &= (1 + \mu)t_s + \eta h_c \end{aligned} \right\} (14)$$

Therefore,

$$h_c = t_s \{1 - (1 + \mu)\beta\} / \eta \quad (15)$$

For a parametric variation of  $\eta$ , plots of  $h_c/t_s$  vs  $\beta$  for symmetric sandwich ( $\mu = 1$ ) and open back ( $\mu = 0$ ) sections are given in Figure 14. It can be seen that

- for a given value of normalized front facesheet thickness  $\beta$ , the open back rib height is greater than the sandwich core depth

- $h_c$  varies linearly with  $\beta$  for a given  $\mu$  and linearly with  $\mu$  for a given  $\beta$
- $h_c$  increases with decrease in core or rib density  $\eta$

It can also be seen from Figure 14 that  $h_c$  becomes zero for some limiting values of  $\beta$ . When this happens, all the available material is required for the facesheets and light-weighting is no longer possible. The limiting value of  $\beta$  is obtained from formula (15) by making  $h_c = 0$  and solving it for  $\beta$ . This yields

$$\beta_{\max} = 1/(1 + \mu) \quad (16)$$

Since  $\mu$  ranges from 0 for the open back to 1 for the symmetric sandwich section,  $\beta_{\max}$  varies from 1/2 to 1.

### Flexural Rigidity

The flexural rigidity is directly proportional to the unit width cross sectional moment of inertia about the neutral axis, the location of which from the front surface can be shown to be given by

$$c_f = t_s \frac{[(1+\mu)\{\eta(1+\mu) - \mu(2-\kappa) + \kappa(1-2\eta)\}\beta^2 + 2\{\mu(1-\kappa) - \kappa(1-\eta)\}\beta + \kappa]}{2\eta\{(1+\mu)(1-\kappa)\beta + \kappa\}} \quad (17)$$

It can also be shown that the unit width moment of inertia of the light-weighted cross section about the neutral axis is given by

$$I = \left. \begin{aligned} &\frac{(1 + \mu^3)t_f^3 + \kappa\eta h_c^3}{12} + \frac{\mu t_f^2 \{(1 + \mu)t_f + 2h_c\}^2}{4\{(1 + \mu)t_f + \kappa\eta h_c\}} \\ &+ \frac{\kappa\eta t_f h_c \{(1 + \mu^3)t_f^2 + 2(1 + \mu^2)t_f h_c + (1 + \mu)h_c^2\}}{4\{(1 + \mu)t_f + \kappa\eta h_c\}} \end{aligned} \right\} (18)$$

The flexural rigidity of the light-weighted cross section is then given by

$$D = EI/(1 - \nu^2) \quad (19)$$

Dividing this by the flexural rigidity of the weight equivalent solid cross section given by formula (10) and using formulas (9) and (18), the normalized flexural rigidity  $\gamma$  can be shown to be given by

$$\gamma = \frac{D}{D_s} = \frac{I}{I_s} = \frac{\kappa^2 + C_1\beta + C_2\beta^2 + C_3\beta^3 + C_4\beta^4}{(k + C_5\beta)\eta^2} \quad (20)$$

where

$$C_1 = 4\kappa(1 - \kappa)(1 + \mu) \quad (21)$$

$$C_2 = 6\{2(1 - \kappa\eta)\mu + \kappa(\kappa + \eta - 2)(1 + \mu)^2\} \quad (22)$$

$$C_3 = 4(1 + \mu)\{3\eta - \kappa\eta^2 - 6\}\mu + \kappa\eta(\eta - 3)(1 + \mu^2) + \kappa(3 - \kappa)(1 + \mu)^2 \quad (23)$$

$$C_4 = (1+\mu)^2 [2\{6(1-\eta) + \eta^2(1+2\kappa)\}\mu + \eta(\eta+6\kappa-4\kappa\eta)(1+\mu^2) - \kappa(4-\kappa)(1+\mu)^2] \quad (24)$$

$$C_5 = (1 - \kappa)(1 + \mu) \quad (25)$$

Formulas (20) through (25) can be used to construct normalized design curves for flexural rigidity as a function of rear facesheet thickness ratio  $\mu$  with a parametric variation of the core (or rib) solidity ratio  $\eta$  for any given value of core effectiveness factor  $\kappa$ , such as 1/2 for the conventional square and triangular rib patterns. Such design curves have two salient features: (a) A maximum value of flexural rigidity for an optimum front facesheet thickness ratio  $\beta_0$ , and (b) a transitional value of  $\beta$  for which the sandwich and open back cross sections have equal flexural rigidities. We need to derive the corresponding equations and will study the ensuing results first.

### Optimization

By differentiating  $\gamma$  given by formula (20) with respect to  $\beta$  and equating the result to zero, we obtain the required equation for optimum  $\beta$  for which  $\gamma$  is a maximum. After simplification, the resulting equation is

$$\left. \begin{aligned} (\kappa C_1 - \kappa^2 C_5) + 2\kappa C_2 \beta_0 + (3\kappa C_3 + C_2 C_5) \beta_0^2 \\ + (4\kappa C_4 + 2C_3 C_5) \beta_0^3 + 3C_4 C_5 \beta_0^4 = 0 \end{aligned} \right\} \quad (26)$$

This equation can be numerically solved for an optimum value of  $\beta$ , which yields the required maximum value of the flexural rigidity ratio  $\gamma$ . For symmetric sandwich cross sections for which  $\mu = 1$  and  $0 < \beta < 0.5$ , eq (26) can be reduced to

$$\begin{aligned} 4(\eta^2 - 3\eta - \kappa + 3)\beta_0^2 \\ + 4(n + \kappa - 2)\beta_0 + (1 - \kappa) = 0 \end{aligned} \quad (27)$$

This can be solved to obtain the following  $\beta_0$  for symmetric sandwich cross sections

$$\beta_0 = \frac{\sqrt{(1-\kappa\eta)} - \sqrt{(1-\eta)}}{2\{\sqrt{(1-\kappa\eta)} - \sqrt{(1-\eta)}\}^3} \quad (28)$$

Based on  $C_1$  through  $C_5$  defined by formulas (21) through (25) respectively, eq (26) was numerically solved for a parametric variation of  $\eta$  and  $\mu$  assuming  $\kappa = 0.5$  for square and triangular rib patterns. The results are shown in Figure 15 as plots of optimum front facesheet thickness  $\beta_0$  vs rear facesheet thickness ratio  $\mu$  for rib density variation between 4 and 20 percent. Also of interest are similar plots for total facesheet thickness ratio  $(1 + \mu)\beta_0$ , shown in Figure 16 and those for core or rib depth ratio  $(h_c/t_s)_0$ , shown in Figure 17. It can be seen from Figures 15 and 16 that

- the optimum front facesheet thickness ratio ranges between 9.6 and 14.5 % of the weight equivalent solid thickness
- the maximum values of  $\beta_0$  occur for nonsymmetric sandwich sections having the rear facesheet thickness approximately equal to 40 % of the front facesheet thickness
- the ranges of  $\beta_0$  for open back and symmetric sandwich sections are not very different from each

other, 9.6 to 10.7 % for the open back and 10.5 to 11.6 % for the symmetric sandwich type

- the total facesheet thickness ratio increases monotonically with  $\mu$ , and ranges between 9.6 % for the open back type at  $\eta = 4$  % to 23.2 % for the symmetric type at  $\eta = 20$  %. It rises rather rapidly between  $\mu = 0$  and 0.5, and then flattens out between  $\mu = 0.5$  and 1.

For optical systems requiring extremely light-weighted high performance mirrors in the 10 to 30 kg/m<sup>2</sup> class, the equivalent solid thickness for some of the common materials ranges from 0.15 inch to 0.64 inch (See figure 7). For the corresponding open back and symmetric sandwich mirrors, facesheet thickness ranges between 0.014 inch and 0.074 inch. For a nonsymmetric sandwich mirror, the front facesheet thickness can be as high as 0.093 inch, but the corresponding rear facesheet thickness is at most 0.037 inch. In general, producing mirror blanks with such thin facesheets is beyond the current state of the art. Producing optimum glass (ULE, Zerodur) mirrors is questionable even at 50 kg/m<sup>2</sup>.

From a study of the optimum rib depth plots of Figure 17, it is observed that the optimum rib depth ratio of the sandwich section is at most about 10 % smaller than that of the open back section for a given core density, the difference being due to the absence of the rear facesheet in the open back design. Also, the actual optimum rib depth at low rib densities and high mirror weight per unit area may become larger than the available depth envelope in some applications.

Using the optimum  $\beta$  calculated above, the corresponding flexural rigidity ratios were computed from formulas (20) through (25) for  $\kappa = 0.5$ ,  $\eta = 0.04$  through 0.20 in 0.01 increments and  $\mu = 0$  through 1 in 0.1 increments. The results are plotted in Figure 18. The curves are more or less flat, indicating that, for a given  $\eta$ , there is only a small difference between the two extremes of light-weight construction, namely, the open back type at  $\mu = 0$  and the symmetric sandwich type at  $\mu = 1$ . Figure 19 gives a plot of flexural rigidity ratio for these two types vs the rib density  $\eta$ . The optimum symmetric sandwich section has only 13.9 % to 15.7 % more flexural rigidity than the optimum open back section.

### Transition Point

It is evident from the above discussion that currently producible mirrors are not optimum with values of  $\beta$  higher than its optimum values. Consequently, more material is required for facesheets and less is available for the rib structure, resulting in decreased flexural rigidity. With continued increase in  $\beta$ , a point is reached, after which it becomes more advantageous to dispense with the rear facesheet completely and use that material for increasing the rib height. This may be defined as the transition point between sandwich and open back designs. At this point, the two designs have equal flexural rigidities. Above it, the open back design is stiffer than the sandwich design. Below it, that phenomenon is reversed. Denoting the transitional value of the front facesheet thickness ratio by  $\beta_t$ , the equation for determining it is obtained by equating the flexural rigidity ratio  $\gamma$  for  $0 < \mu \leq 1$  to that for  $\mu = 0$ . Using formulas (20) through (25) and performing the necessary algebraic manipulations, the following equation is obtained for the transitional  $\beta$ .

$$\left. \begin{aligned}
& [C_4(1-\kappa) - C_5\{\eta^2(1-4\kappa) + 6\kappa\eta + \kappa(\kappa-4)\}]\beta_t^4 \\
& + [C_3(1-\kappa) + C_4\kappa - 4C_5\kappa(\eta^2-3\eta+3-\kappa) \\
& - \kappa\{\eta^2(1-4\kappa) + 6\kappa\eta + \kappa(\kappa-4)\}]\beta_t^3 + \{C_2(1-\kappa) \\
& + C_3\kappa - 6C_5\kappa(\eta+\kappa-2) - 4\kappa^2(\eta^2-3\eta+3-\kappa)\}\beta_t^2 \\
& + \{C_1(1-\kappa) + C_2\kappa - 4C_5\kappa(1-\kappa) - 6\kappa^2(\eta+\kappa-2)\}\beta_t \\
& + 3\kappa^2(1-\kappa)\mu = 0
\end{aligned} \right\} (29)$$

For  $\kappa = 0.5$ , eq (29) was numerically solved for a parametric variation of  $\eta$  between 0.04 and 0.20 and that of  $\mu$  between 0 and 1. The ensuing transitional values of  $\beta$  are plotted vs  $\mu$  for several values of  $\eta$  in Figure 20. Similar plots of corresponding flexural rigidity are given in Figure 21. It can be seen that

- the transitional  $\beta$  decreases monotonically with increase in  $\mu$
- the dependence of  $\beta_t$  on core density  $\eta$  is only moderate
- transitional  $\beta$  for symmetric sandwich section is approximately twice the corresponding optimum values, that is,  $0.23 < \beta_t < 0.27$  approximately

Again considering the 10 to 30 kg/m<sup>2</sup> class of light-weighted mirrors, for which the weight-equivalent solid thickness ranges from 0.15 inch to 0.64 inch for some of the common mirror materials (See figure 7), the transitional front facesheet thickness ranges between 0.035 inch and 0.173 inch. Such thicknesses are still marginal and risky, except for hot isostatically pressed beryllium for which the facesheet thickness may be as low as 0.080 inch. Therefore, for designs driven by considerations of producibility and maximum achievable stiffness, the open back section may be superior to the symmetric and non-symmetric sandwich sections in many applications at the present time and indeed in the foreseeable future.

For convenience, plots of transitional rib depth ratio  $(h_c/t_s)_t$  vs the rear facesheet thickness ratio  $\mu$  are given in Figure 22 for core density variation between 4 and 20 %.

### Flexural Rigidity Charts

For conventionally light-weighted cores with square, hexagonal or triangular rib patterns, the core effectiveness factor  $\kappa$  equals 1/2. For this value of  $\kappa$ , the flexural rigidity ratio  $\gamma$  was computed at  $\mu = 0, 1/4, 1/2, 3/4$  and 1 for a parametric variation of  $\eta$  between 0.04 and 0.20 in increments of 0.01 and that of  $\beta$  between 0 and 1 in increments of 0.1. The results are plotted in the form of parametric curves of  $\gamma$  vs  $\beta$  for various values of  $\eta$  in Figure 23 for  $\mu = 0$  (open back section), in Figures 24, 25 and 26 for  $\mu =$

1/4, 1/2 and 3/4 respectively (nonsymmetric sandwich sections), and in Figure 27 for  $\mu = 1$  (symmetric sandwich section).

Also shown in each of the above set of curves are loci of optimum and transitional values of  $\beta$ . There are four loci of transitional  $\beta$  shown in Figure 23 for the open back section curves corresponding to the transition points between the open back and each of the four sandwich types considered. The same four loci occur separately in Figures 24 through 27 for the respective sandwich section curves. To the right of a given transition locus, the open back section has more flexural rigidity for any given values of  $\beta$  and  $\eta$  than the sandwich section, whose facesheet thickness ratio is given by the indicated value of  $\mu$ . This phenomenon is reversed for any given values of  $\beta$  and  $\eta$  on the left side of a transition locus.

It can be observed from these curves that the flexural rigidity ratio becomes 1 at the limiting value of  $\beta$  defined by formula (16). This should intuitively be the minimum value of  $\gamma$ , except for some slightly lower values observed between  $\beta = 0.9$  and  $\beta = 1$  for  $\mu = 0$ . This is explained by the fact that the loss in flexural rigidity resulting from the rib effectiveness factor  $\kappa$  being equal to only 1/2 is more than the gain made from the very small rib heights available in that range of  $\beta$ . However, this is of academic interest only, because no practical light-weighting is imaginable in that range.

### Conclusion

This concludes our study of normalized flexural rigidity characteristics of light-weighted mirrors independently of material properties. The normalization was achieved by means of weight-equivalent solid thickness of the mirror. There are two main conclusions derived from the study.

- Optimum light-weighting required for maximization of flexural rigidity is beyond the present state of art of the fabrication technology.
- There is a transition point in the front facesheet thickness ratio, above which the open back light-weighting is structurally superior to the sandwich type of light-weighting.

All of the graphical data presented in this technical memorandum are based on the core (or rib) effectiveness factor of 1/2, applicable to conventionally light-weighted cores having square or triangular rib patterns. However, the equations are applicable to light-weighting with other values of  $\kappa$ . For example,  $\kappa$  for hexagonal rib patterns and for foamed types of cores made from the parent or other materials is significantly less than 0.5. With appropriate values of  $\kappa$  in such cases, the above equations can be used for a similar study or a point design.

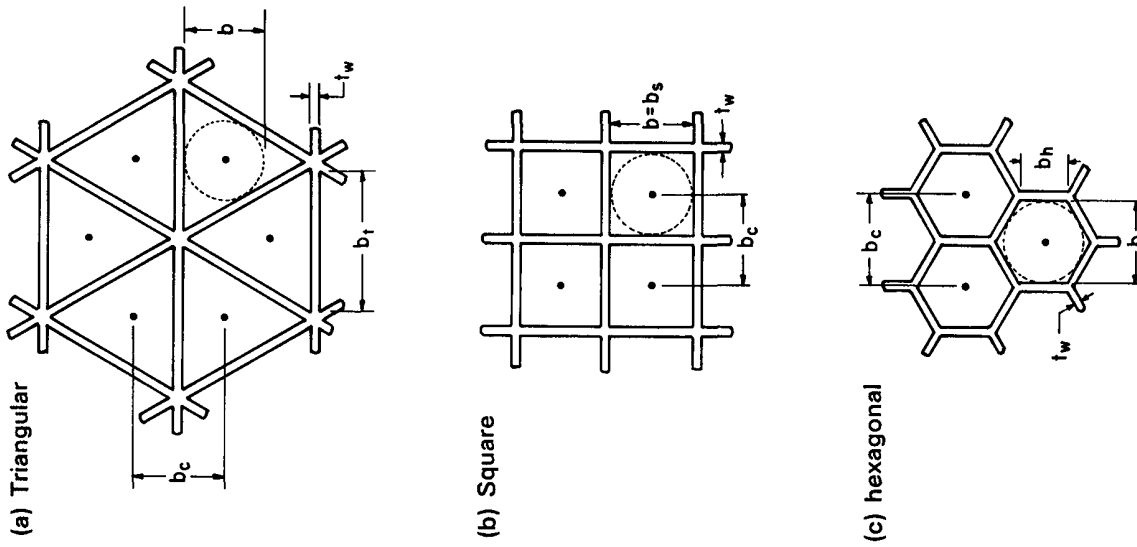


Figure 2. Several types of rib patterns

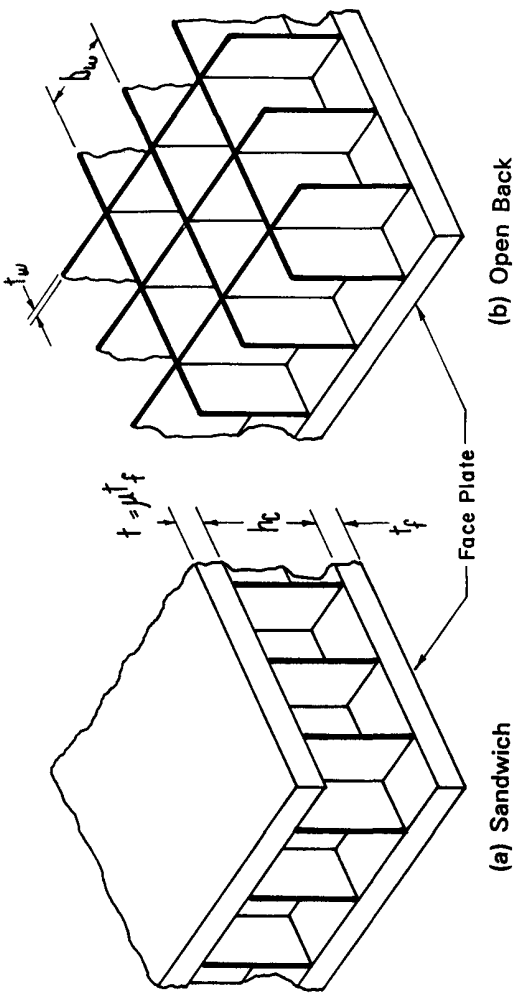


Figure 1. Light-weighted mirror configurations with square rib pattern

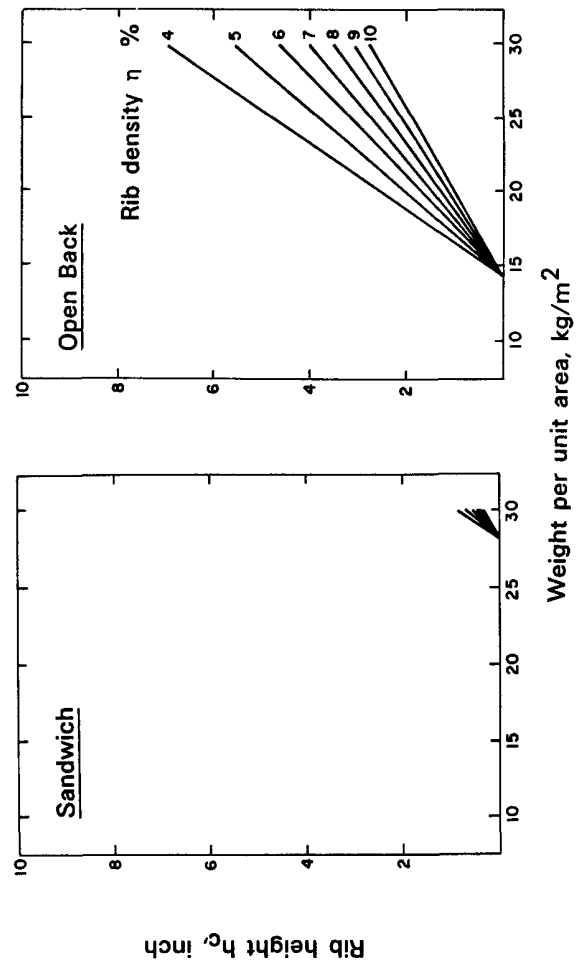


Figure 3. Variation of rib height with weight per unit area and rib density for ULE mirrors when  $t_f = 0.25$  inch

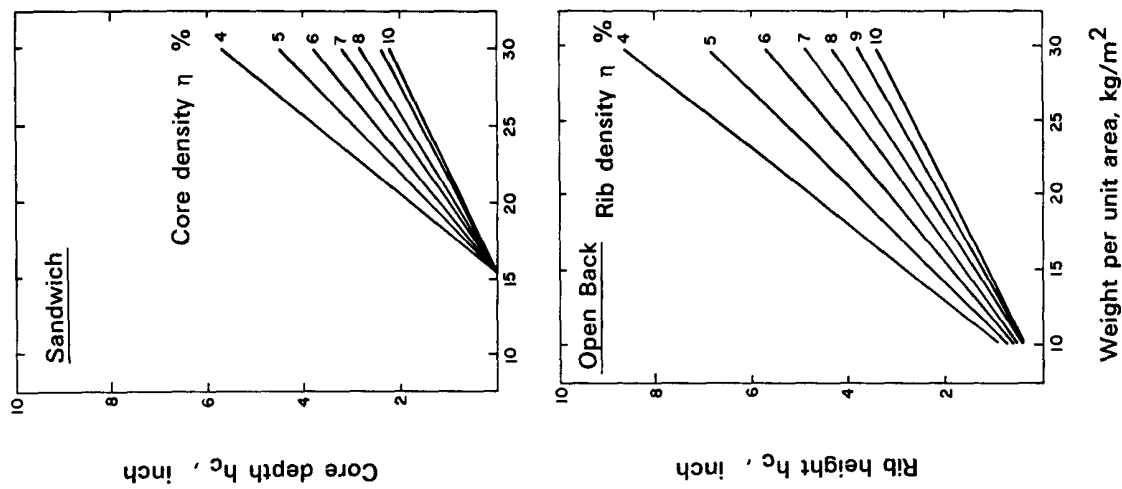


Figure 4. Variation of core depth and rib height with weight per unit area and rib density for Zerodur mirrors when  $t_f = 0.12$  inch

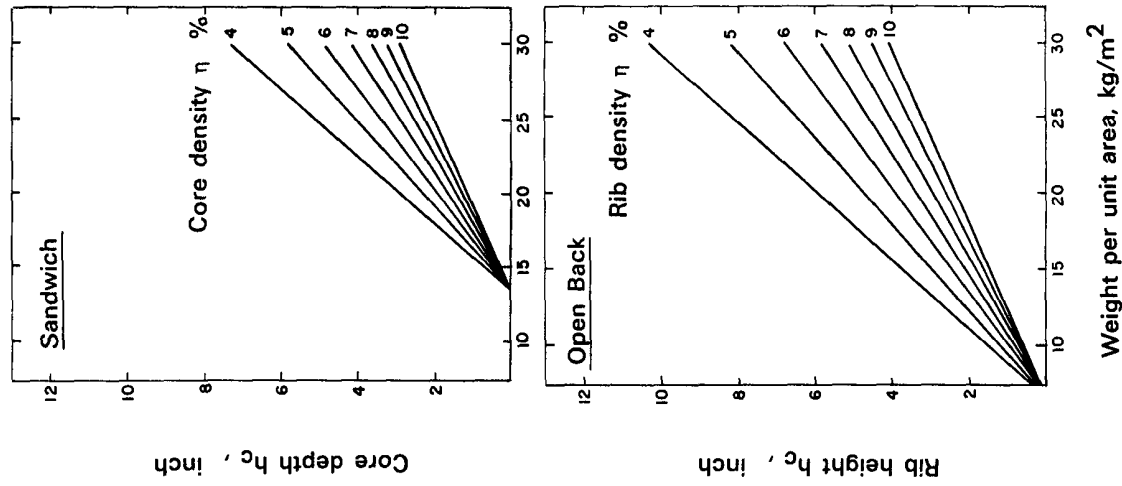


Figure 5. Variation of core depth and rib height with weight per unit area and rib density for Heraeus Fused Silica mirrors when  $t_f = 0.12$  inch

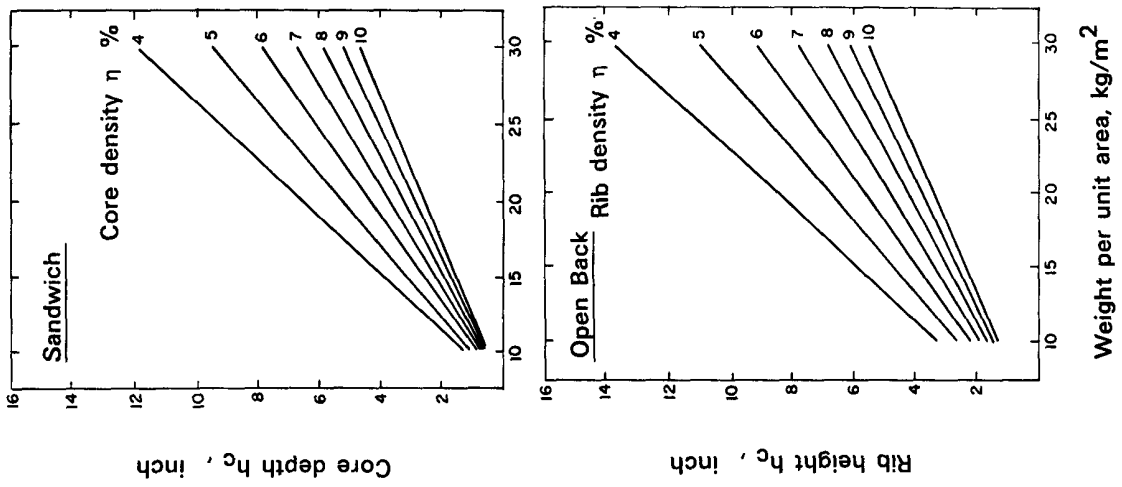


Figure 6. Variation of core depth and rib height with weight per unit area and rib density for Beryllium mirrors when  $t_f = 0.08$  inch



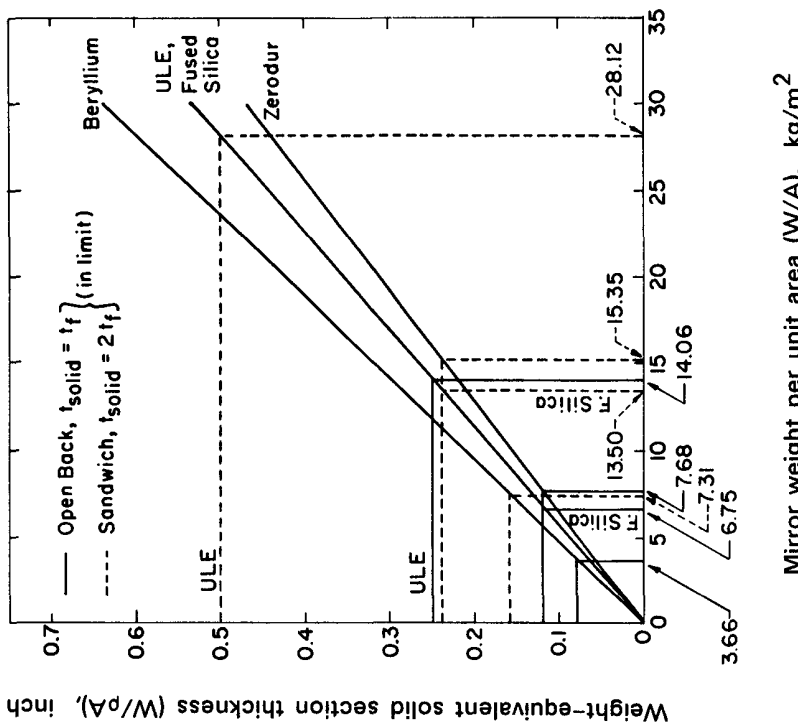


Figure 7. Variation of weight equivalent solid cross section thickness with mirror weight per unit area and limits of light-weighting for the assumed state-of-the-art fabrication constraints on facesheet thickness

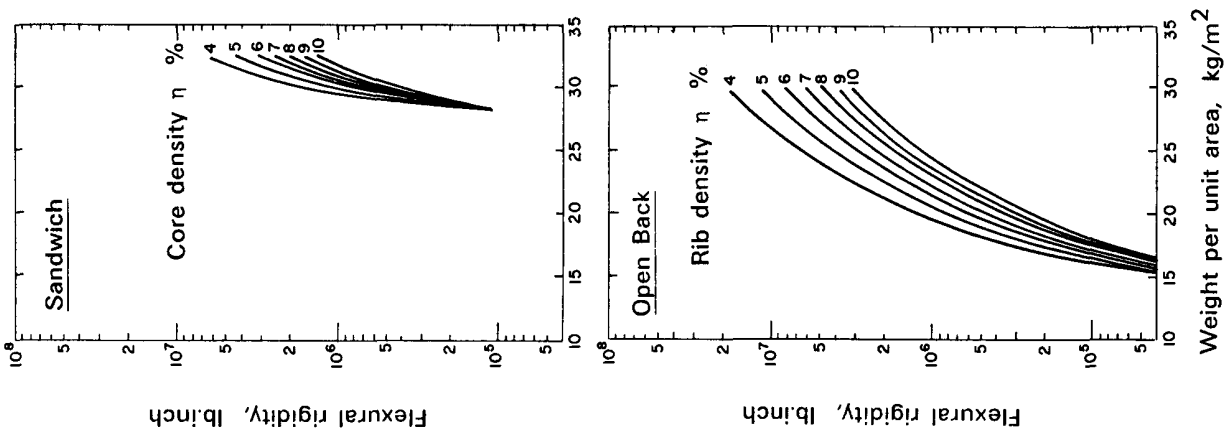


Figure 8. Flexural rigidity charts for ULE mirrors with  $t_f = 0.25$  inch

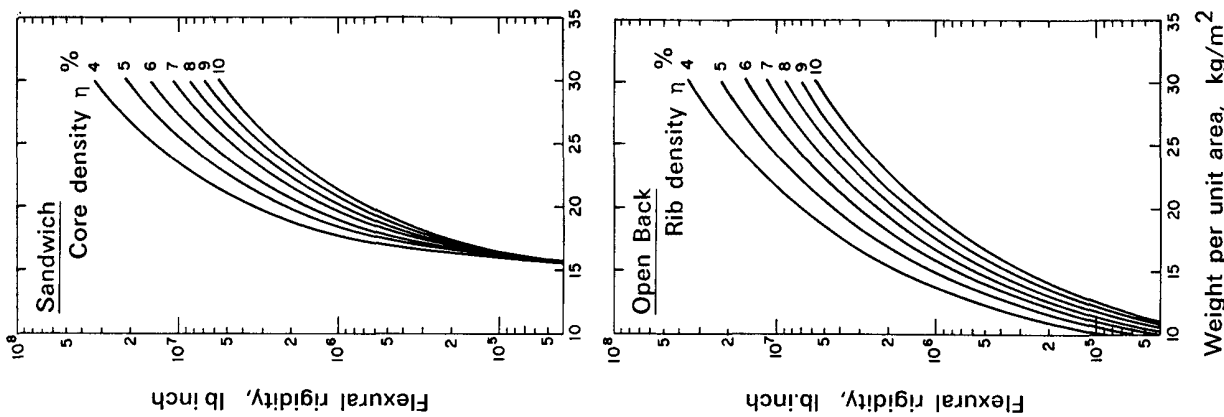


Figure 9. Flexural rigidity charts for Zerodur mirrors with  $t_f = 0.12$  inch

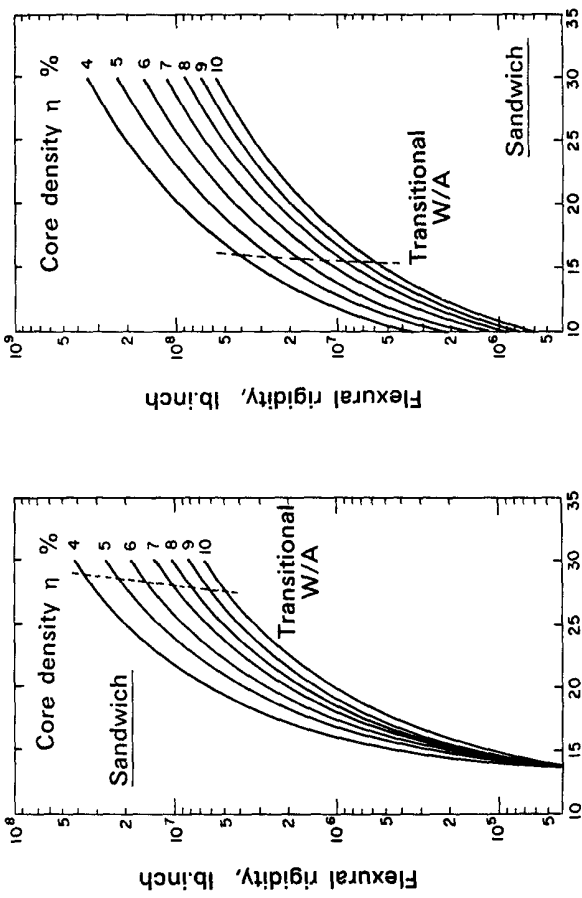


Figure 10. Flexural rigidity charts for Heraeus fused silica mirrors with  $t_f = 0.12$  inch

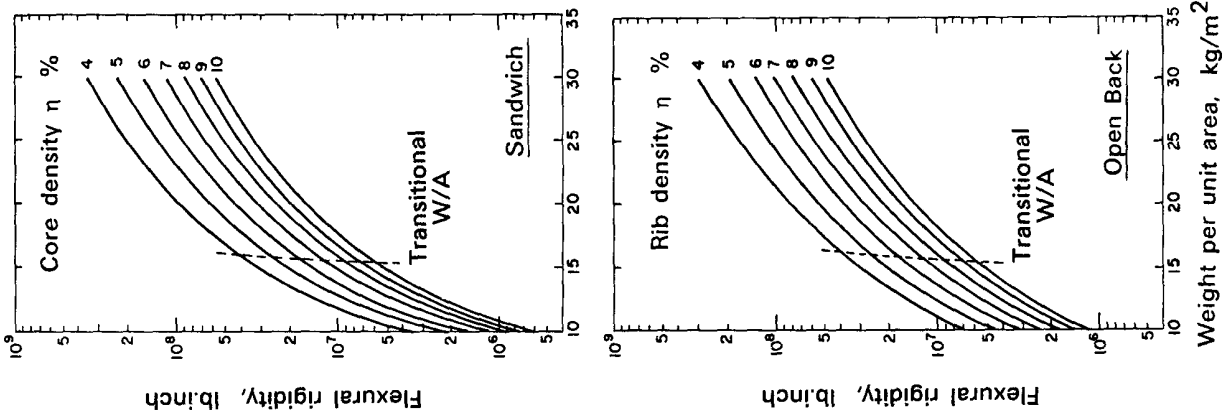


Figure 11. Flexural rigidity charts for Beryllium mirrors with  $t_f = 0.08$  inch

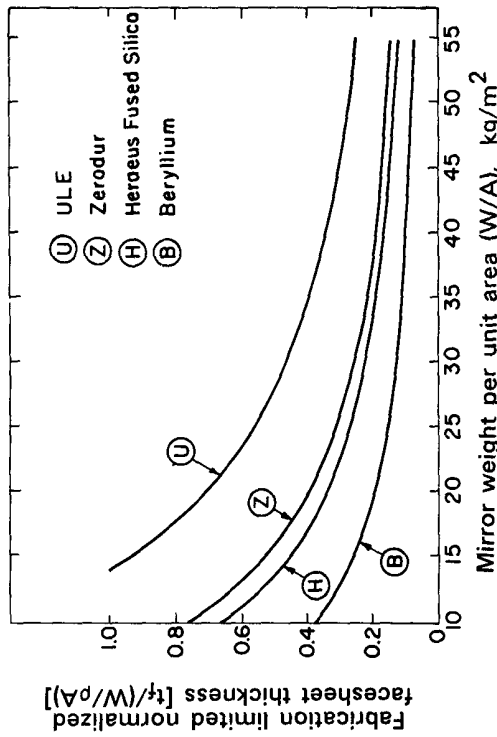


Figure 12. Variation of fabrication limited normalized facesheet thickness with mirror weight per unit area

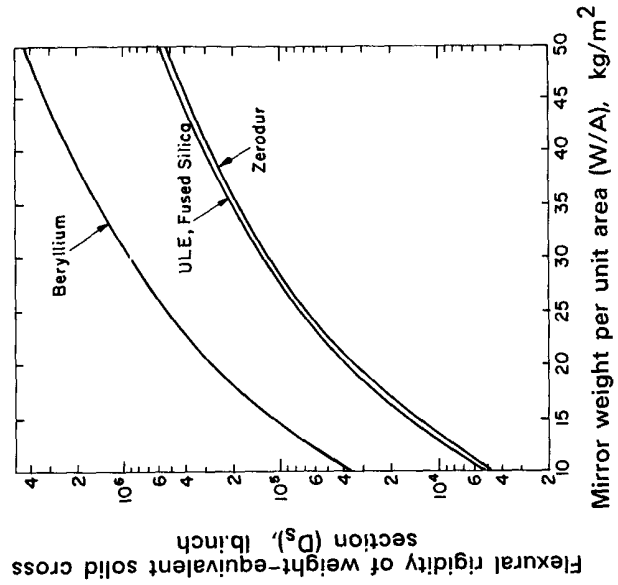


Figure 13. Variation of weight-equivalent solid section flexural rigidity for several mirror materials with weight per unit area

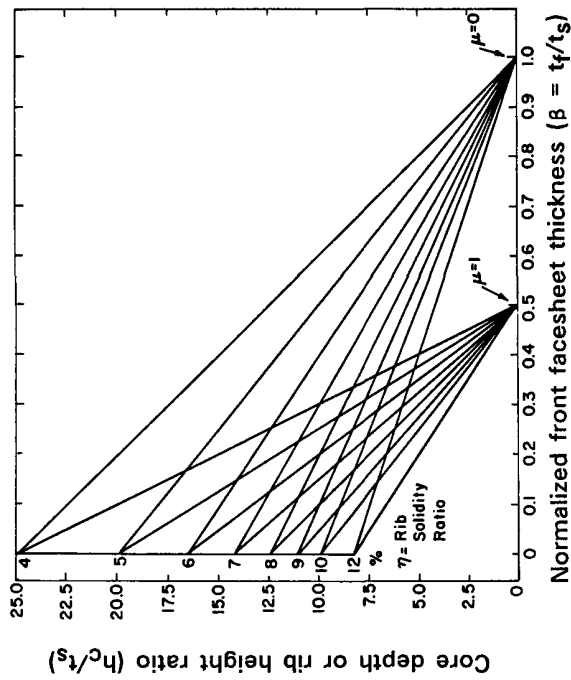


Figure 14. Core depth or rib height chart for sandwich ( $\mu = 1$ ) and open back ( $\mu = 0$ ) configurations

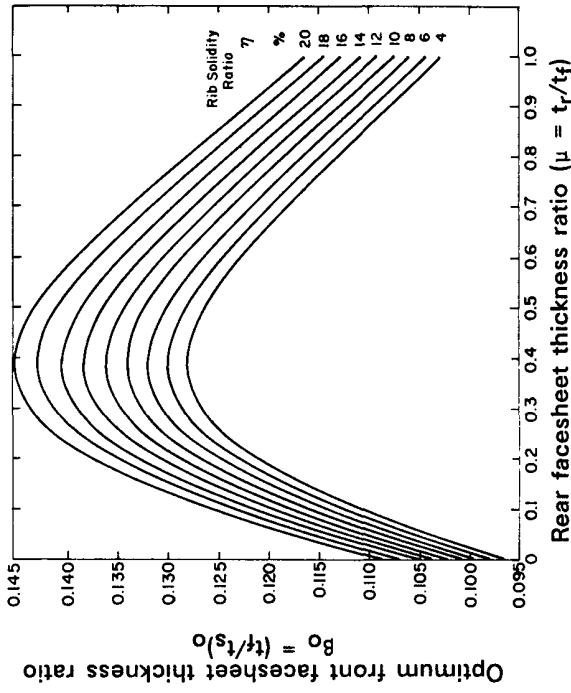


Figure 15. Variation of optimum front facesheet thickness ratio with rear facesheet thickness ratio and rib solidity ratio

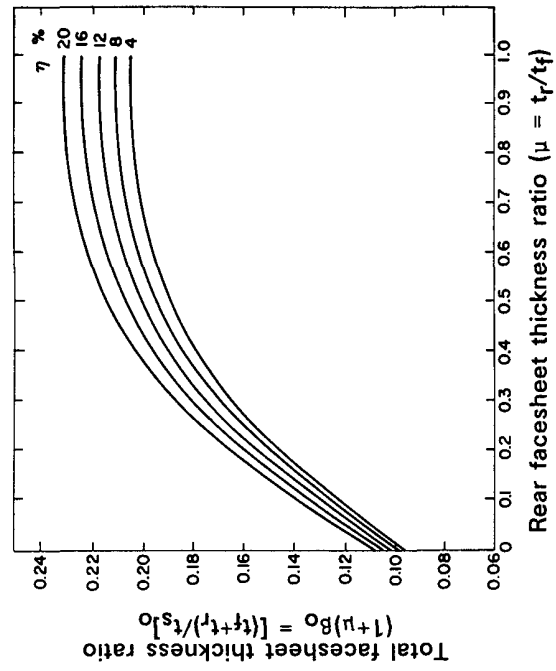


Figure 16. Variation of total facesheet thickness ratio with rear facesheet thickness ratio and rib solidity ratio

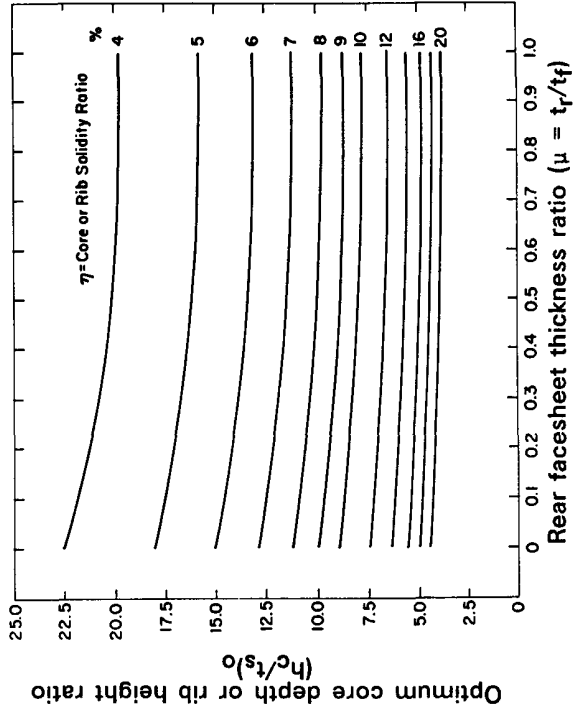


Figure 17. Variation of optimum core depth or rib height ratio with rear facesheet thickness ratio and rib solidity ratio

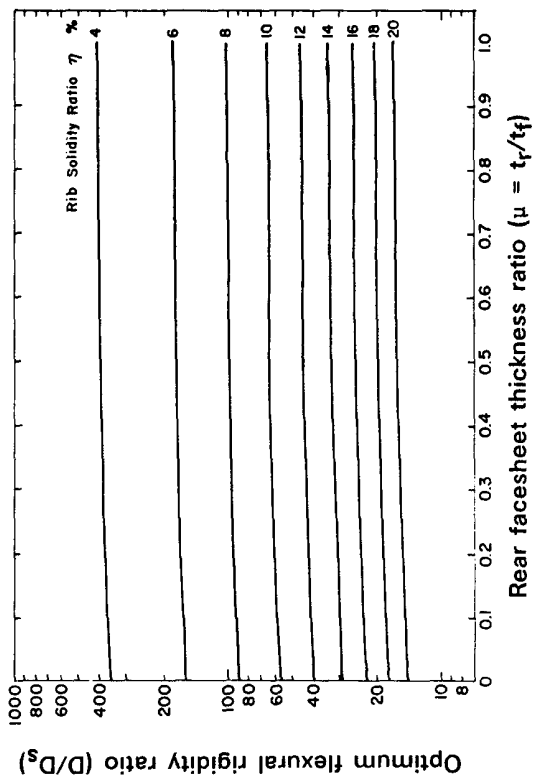


Figure 18. Variation of optimum flexural rigidity ratio with rear facesheet thickness ratio and rib solidity ratio

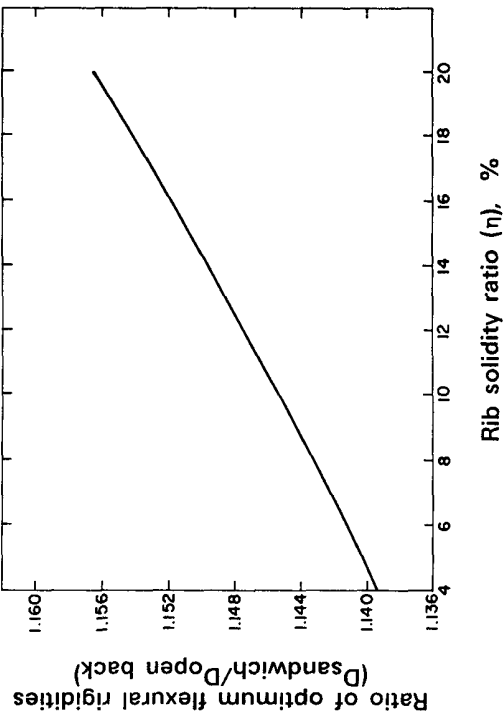


Figure 19. Variation of the ratio of optimum flexural rigidities of sandwich and open back configurations with rib density

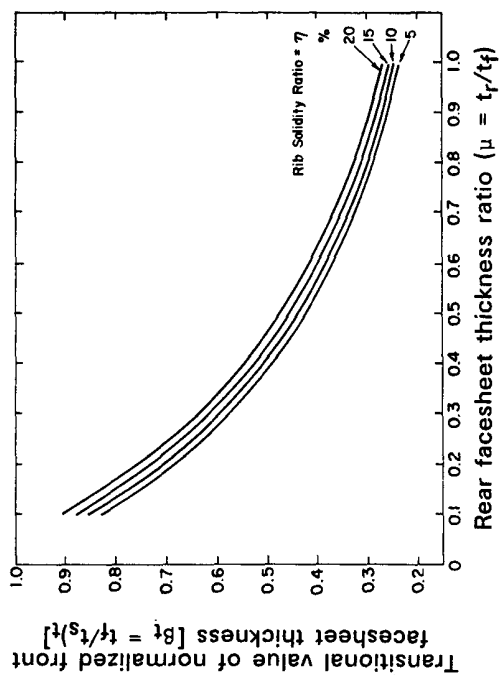


Figure 20. Variation of transitional front facesheet thickness ratio with rear facesheet thickness ratio and rib solidity ratio

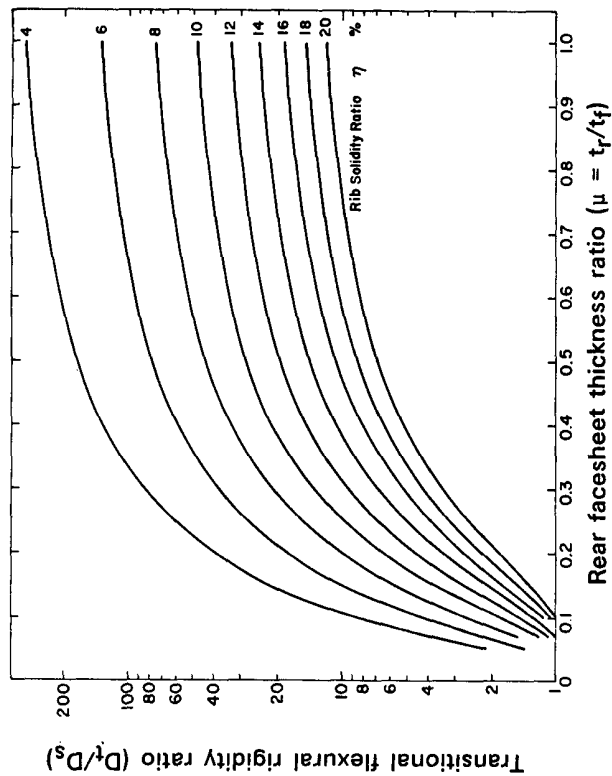


Figure 21. Variation of transitional flexural rigidity ratio with rear facesheet thickness ratio and rib solidity ratio

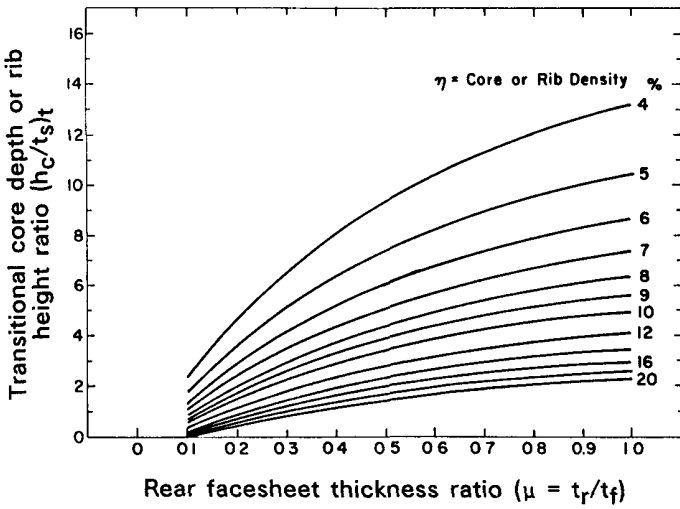


Figure 22. Variation of transitional core depth or rib height ratio with rear facesheet thickness ratio and rib solidity ratio

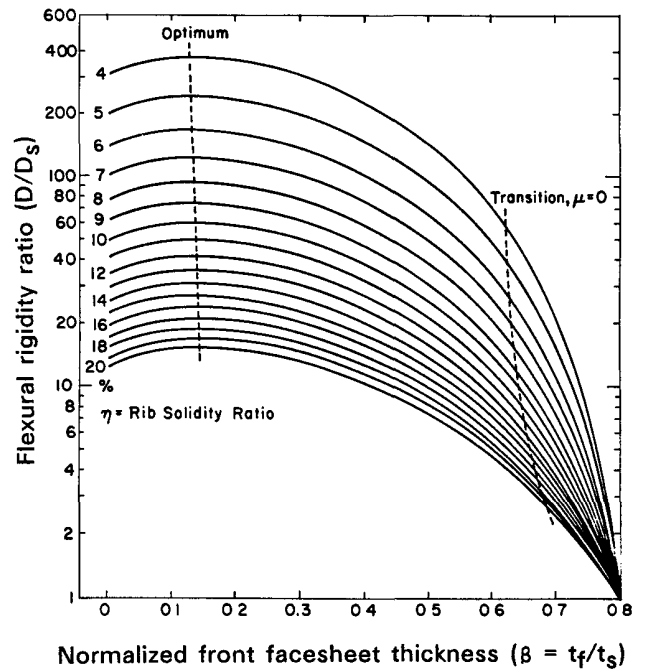


Figure 24. Flexural rigidity chart for nonsymmetric sandwich configurations ( $\mu = 1/4$ )

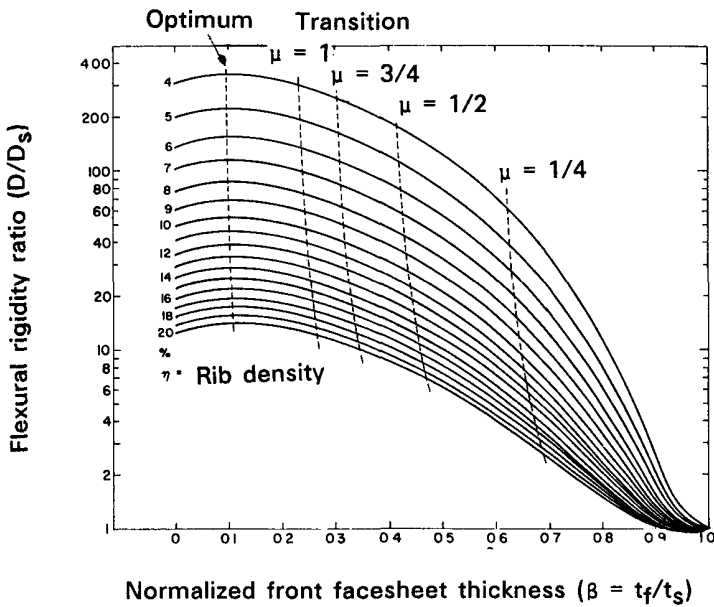


Figure 23. Flexural rigidity chart for open back configurations ( $\mu = 0$ )

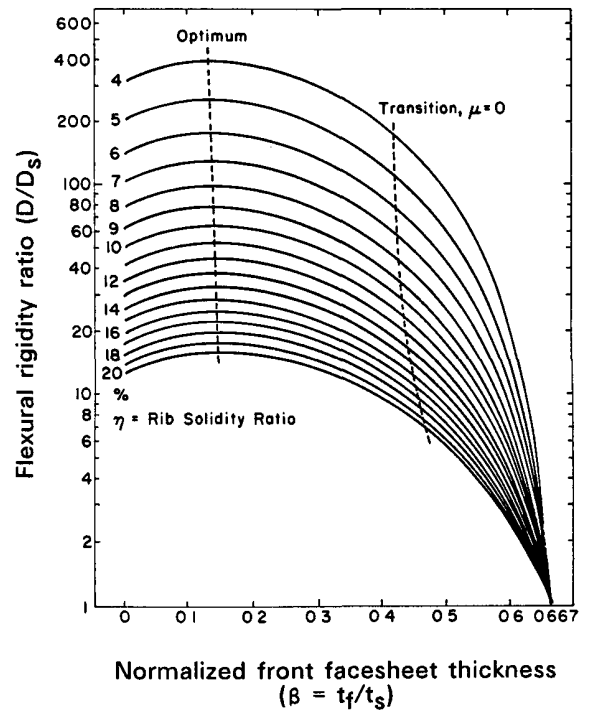


Figure 25. Flexural rigidity chart for nonsymmetric sandwich configurations ( $\mu = 1/2$ )

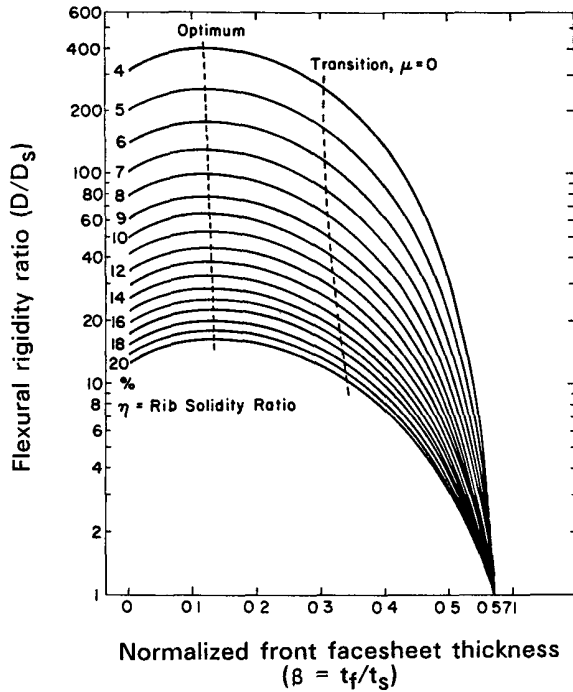


Figure 26. Flexural rigidity chart for nonsymmetric sandwich configurations ( $\mu = 3/4$ )

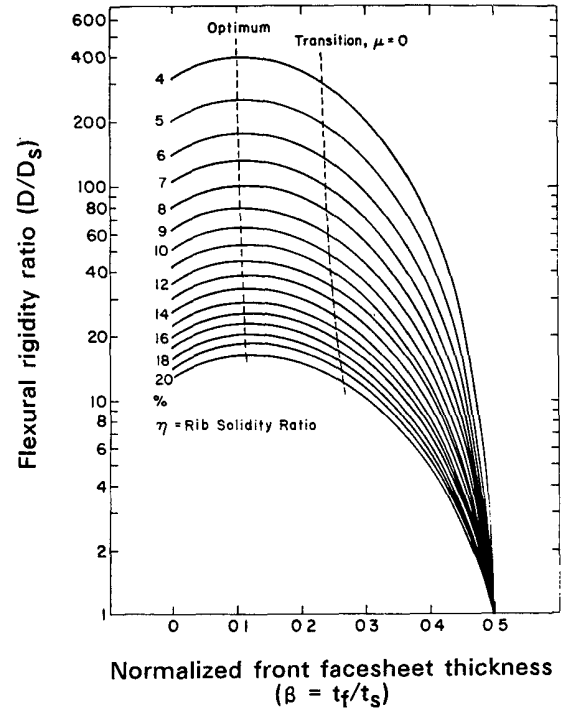


Figure 27. Flexural rigidity chart for symmetric sandwich configurations ( $\mu = 1$ )

### Appendix : Core Density

It is of interest to note that the core density for square, hexagonal and triangular rib patterns (Figure 2) can be expressed by a single formula based on the diameter of the inscribed circle and rib thickness as follows.

$$\eta = \frac{(2b + t_w)t_w}{(b + t_w)^2} \quad (A.1)$$

where  $b_s = b$ ,  $b_t = \sqrt{3}b$  and  $b_h = b/\sqrt{3}$ . The lengths  $b_s$ ,  $b_t$  and  $b_h$  are associated with the hollow pockets of the core, which the inscribed circle of diameter  $b$  is referred to above. Since  $(b + t_w)$  in formula (A.1) equals the center to

center rib spacing  $b_c$ , formula (A.1) may also be written as

$$\eta = \frac{(2b_c - t_w)t_w}{b_c^2} \quad (A.2)$$

For equal core density rib patterns with a given  $t_w$ , we have

$$b_s = \sqrt{3}b_h = b_t/\sqrt{3} \quad (A.3)$$

The sketches of Figure 2 are more or less scaled to illustrate the three equal core density rib patterns in accordance with formulas (A.3). The center to center spacing or cell pitch is the same for all three patterns. So also are diameters of the inscribed circles

### Acknowledgement

The work presented in this paper was performed under internal support from the Perkin-Elmer Corporation.